ELSEVIER

Available online at www.sciencedirect.com

ScienceDirect

Procedia Engineering 8 (2011) 280–285

Engineering Procedia

2nd International Science, Social Science, Engineering and Energy Conference 2010: Engineering Science and Management

An Analytical Model for Detectivity Prediction of Uncooled Bolometer Considering all Thermal Phenomena Effects

Hamed Azari Najafabadi[a,]*, Asghar Asgari[b], Manouchehr Kalafi[c], Khadije Khalili[a]

[a]*Photonics-Electronics Group, Research Institute for Applied Physics and Astronomy, The University of Tabriz, Tabriz 51665-163, Iran*

[b]*School of Electrical, Electronic and Computer Engineering, The University of Western Australia, Crawley, WA 6009, Australia*

[c]*Department of Solid State Physics, Faculty of Physics, The University of Tabriz, Tabriz 51665-163, Iran*

Elsevier use only: Received 15 November 2010; revised 15 December 2010; accepted 20 December 2010

Abstract

In this paper, we proposed an approach for analyzing uncooled infrared bolometer detector. The model is taken into account temperature dependence of Thermal Coefficient of Resistance (TCR), thermal capacitance and thermal conduction through legs. Radiation thermal conductance between bolometer membrane and its surrounding is defined based on Stefan-Boltzmann radiation law. Calculations were carried out using an equivalent thermal circuit. Eventually, the Detectivity is obtained as figure of merit, considering temperature fluctuation noise. By this analysis, we achieved a reliable method to estimate the performance of bolometer detector in comparison with experimental cases.

Keywords: Detectivity; Equivalent thermal circuit; Stefan-Boltzmann radiation law; Temperature coefficient of resistance (TCR)

1. Introduction

Bolometer detectors have become choice of technology because of their low-cost infrared imaging systems, beside their room temperature performance. Some of the most common commercial infrared imaging applications are night vision, fire fighting, industrial process control (non destructive test), medical imaging, mine detection and thermography.

At present work, we used a precise equation for resistance as a function of temperature which results in an accurate temperature dependence of Thermal Coefficient of Resistance (TCR). For more reliable results, we considered temperature dependence of thermal capacitance and thermal conduction through legs. Radiation Thermal Conductance calculations were carried out using Stefan-Boltzmann radiation law. Incident power from image object was appeared in equivalent thermal circuit through a conductance between image object and bolometer membrane.

* Corresponding author. Tel.: +66-42-772-391; fax: +66-42-772-392
E-mail address: *h.azari87@ms.tabrizu.ac.ir*

doi:10.1016/j.proeng.2011.03.052

We chose Detectivity as figure of merit for our model and obtained its value in a good agreement with practical cases.

2. Thermal Model

Detector Unit Element Structure. Fig. 1 shows the bolometer structure which is a conventional resonant optical cavity bolometer detector unit [1] that two support legs suspending bolometer membrane above detector base (DB). Manufacturing long legs with small cross-sectional area, using materials with low thermal conductivity, is one of the major issues in bolometer technology.

Many types of VO_x material with different operating temperature ranges and TCR, depending on what and how much materials are mixed and what fabrication process is used, are employed most widely as bolometer membrane material. Our calculation model is based on VO_2 material as bolometer membrane with a 26 kΩ resistance and 0.02 1/K TCR at room temperature [2]. Typical operating temperature range for this kind of material is about 296-323 K.

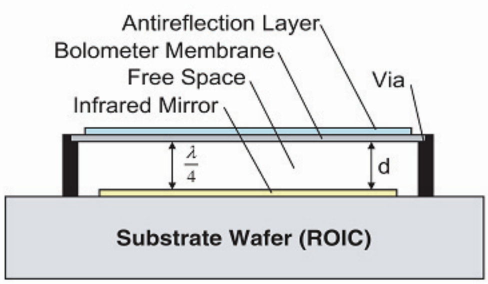

Fig. 1. Cross-sectional image of bolometer design with resonant optical cavities for high absorption of the incident infrared radiation.

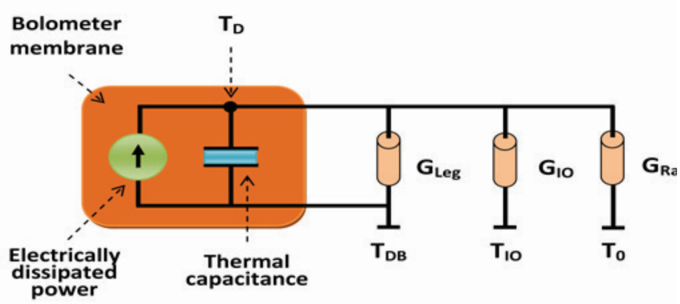

Fig. 2. Equivalent thermal circuit. G_X is thermal conductance between bolometer membrane and thermal element X which is in temperature T_X.

Thermal Effects. In addition to electrically dissipated power generated inside the bolometer membrane due to applied bias, energy exchange between bolometer membrane and its surrounding occurs through conduction.

Different kinds of conduction are included in total thermal conduction. First of all is thermal conduction between the bolometer membrane and detector unit base in temperature T_{DB} through legs. Another thermal conduction occurs between bolometer membrane and other thermal elements due to radiation energy exchange. With regard to our configuration, in addition to radiation thermal conduction (RTC) between bolometer membrane and Image Object (IO), RTC will happen between bolometer membrane and its surrounding which is in temperature T_0.

Thermal Equivalent Circuit. Based on previous discussion, the equivalent thermal circuit for our configuration can be shown as Fig. 2. In this analysis, the gas pressure inside the detector vessel is assumed to be less than 0.1 mbar and consequently thermal conduction through the gas is negligible. Meanwhile, detector base temperature (T_{DB}) can be kept in a fixed value and controlled, using a Thermo-Electric module.

Heat Balance Equation. For this equivalent thermal circuit we can obtain the following equations.

$$W_{Leg} = G_{Leg} \cdot (T_{DB} - T_D) \quad (1)$$

$$W_{IO} = G_{IO} \cdot (T_{IO} - T_D) \quad (2)$$

$$W_{Rad} = G_{Rad} \cdot (T_D - T_0) \quad (3)$$

where W_X is the energy flow through thermal conductance G_X. In steady state condition, the power flowing into the bolometer membrane is equal to the out flowing power, thus

$$W_{IO} + E_d = W_{Rad} + W_{Leg} \quad (4)$$

where E_d is electrically dissipated power in bolometer membrane.

The bolometer membrane temperature (T_D) at any time t can be achieved by solving refined heat balance equation (5) to give Eq. (6).

$$C\frac{dT_D}{dt}+G_{Rad}\cdot(T_D-T_0)+G_{Leg}\cdot(T_{DB}-T_D)=G_{IO}\cdot(T_{IO}-T_D)+E_d \tag{5}$$

$$T_D=\frac{\tau}{C}\cdot[(G_{IO}\cdot T_{IO}+G_{Rad}\cdot T_0+G_{Leg}\cdot T_{DB}+E_d)+\Delta T\cdot G_{IO}\cdot\{1-\exp(-t/\tau)\}] \tag{6}$$

where

$$\tau=C/G_{IO}+G_{Rad}+G_{Leg} \tag{7}$$

is the system time constant and ΔT is the temperature change of image object after initial time t=0.

Thermal equivalent circuit and subsequent heat balance equation show that if thermal conductance through support legs became zero as an ideal model, all energy exchanges with the bolometer membrane are radiative. In such situation bolometer detector operates in a background limited mode.

3. Thermal Parameters

Thermal Conductance through Legs : Temperature dependence of thermal conductance of a thermal link between two elements at temperatures T and T_x can be expressed [3] as

$$G_{Leg}=G_{Leg}(T,T_x)=\frac{G_{Leg_0}}{\beta+1}\cdot\left[\frac{(T/T_x)^{\beta+1}-1}{T/T_x-1}\right] \tag{8}$$

where G_{Leg_0} is thermal conductance in $T\rightarrow T_x$ and β is constant.

Radiation Thermal Conductance: Based on Stefan-Boltzmann radiation law, radiation thermal conductance between bolometer membrane with area A_D and emissivity ε_D in temperature T_D and its surrounding is expressed by [4]

$$G_{Rad}=4\sigma\cdot\varepsilon_D\cdot A_D\cdot T_D^3 \tag{9}$$

where σ is Stefan-Boltzmann constant.

Incident Power from image Object: Incident power from image object was considered in equivalent thermal circuit through a conductance between image object and bolometer membrane (G_{IO}). Radiation thermal conductance between the image object and detector membrane through an optical system can be expressed by [5]

$$G_{IO}=\frac{A_D}{4F^2+1}\int_{\lambda_1}^{\lambda_2}\tau_{O\lambda}\cdot[\varepsilon_{IO}\cdot\eta_D\cdot W_\lambda(T_{IO})-\varepsilon_D\cdot\eta_{IO}\cdot W_\lambda(T_D)]\cdot d\lambda/[T_{IO}-T_D] \tag{10}$$

where

$$W_\lambda(T)=\frac{2hc^2}{\lambda^5}\frac{1}{\exp(hc/\lambda K_BT)-1} \tag{11}$$

is Plank's blackbody radiation law and other parameters meaning and their typical values are listed in Table 1.

Thermal Capacitance. However thermal capacitance of bolometer membrane frequently considers as a constant, but for precise calculations can be expressed as a power law function of temperature [6].

$$C=C(T)=C_0T^{\beta_c} \tag{12}$$

where C_0 and β_c are constant.

Resistance and Temperature Coefficient of Resistance. Temperature dependence of resistance and temperature coefficient of resistance which is defined by Eq. (13) are two major parameters of bolometer membrane material.

$$TCR=\frac{1}{R}\frac{dR}{dT} \tag{13}$$

where R is resistance at temperature T. If we use Eq. (14) for temperature dependece of resistance [3],

$$R(T)=R^*\exp\sqrt{\frac{T_g}{T}} \tag{14}$$

where T_g is a material parameter and R^* depends on both material and membrane geometry. Thus, TCR can be extracted from Eq. (14), using Eq. (13).

$$TCR = -\frac{1}{2}\frac{T_g^{\,1/2}}{T^{\,3/2}} \tag{15}$$

4. Bolometer Performance Prediction

Bolometer Membrane Temperature: In order to obtaining initial bolometer membrane temperature, Eq. (6) should be solved in steady state condition (t=0). For this purpose we used the proposed Eqs. in previous section. Thermal conductance of support legs was calculated based on Eq. (8) using β=1 as used for a metallic thermal link [3]. Constant parameter T_g and R^* in Eq. (14) were extracted from room temperature values of resistance and TCR for a typical bolometer detector material.

Typical bolometer detector parameters in Table 1 and the self consistent method were applied for obtaining initial value of bolometer membrane temperature; this value and other output parameters are listed in table 2. Equality of total inflow power to the bolometer membrane and the total outflow power from it, in steady state, shows our method validity. Responsivity of bolometer detector is shown in Fig. 3, based on Eq. (6) when temperature of image object changes 20° suddenly.

Table 1: Input Parameters Meaning and Values

Symbol	*Meaning*	*Value and Unit*
F	F number of optical system	1.5
λ_1	Short Wavelength Cut-off	8×10^{-6} [m]
λ_2	Long Wavelength Cut-off	14×10^{-6} [m]
$\tau_{O\lambda}$	Transmittance of Optical System	0.9
ε_{IO}, η_{IO}	Emissivity and Absorptance of Image Object	0.8
ε_D, η_D	Emissivity and Absorptance of Detector Membrane	0.9
h	Plank constant	6.62×10^{-34} [J.s]
c	Light speed	3×10^{8} [m/s]
σ	Stefan-Boltzmann Costant	5.67×10^{-8} [J/s.m.K
K_B	Boltzmann constant	1.38×10^{-23} [J/K]
T_{IO}	Temperature of Image Object	303 [K]
T_{DB}	Temperature of Detector Base	300 [K]
A_D	Area of Detector Membrane	5.61×10^{-10} [m^2]
G_{Leg0}	Thermal Conductance through Leg	3.75×10^{-8} [W/K]
C (298° K)	Thermal Capacitance	5×10^{-10} [J/K]
β_c	Constant Power of T in Eq. (12)	1.2
R (298° K)	Resistance	2.6×10^{4} [Ω]

Table 2: Output Parameters Values

Parameter	*Value*
Inflow Radiation Power from Image Object	1.74×10^{-8} [W]
Electrically Dissipated Power	2.49×10^{-8} [W]
Total Inflow Power	4.22×10^{-8} [W]
Outflow Radiation Power to Image Object	1.67×10^{-8} [W]
Outflow Power Through Support Legs	1.85×10^{-8} [W]
Outflow Power Through Radiation	6.96×10^{-9} [W]
Total Outflow Power	4.22×10^{-8} [W]
Thermal Conductance between Image Object and Bolometer Membrane (G_{IO})	2.26×10^{-10} [W/K
Thermal Conductance Through Support Legs (G_{Leg})	7.53×10^{-8} [W/K
Radiation Thermal Conductance between Bolometer Membrane and its Surrounding (G_{rad})	3.10×10^{-9} [W/K
Total Thermal Conductance	7.86×10^{-8} [W/K
Temperature of Bolometer Membrane (T_D)	300.24 [K]
Time System Constant (τ)	0.00641 [s]

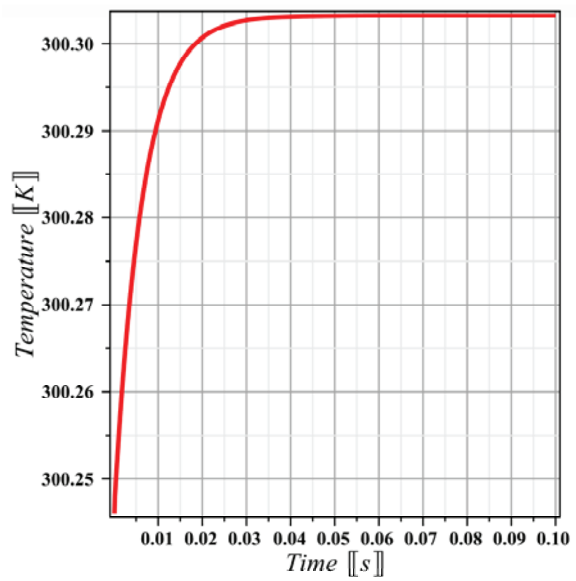

Fig. 3. Response curve of bolometer detector model

Figure of Merit. The most important noise effects that involve bolometer performance are thermal fluctuation noise, Johnson noise and 1/f noise whereas read-out integrated circuit (ROIC) related noise leaves aside for electronic engineering designer. Ordinarily, Johnson noise contributing part can be neglected compared with two other noise types over the frequency range in which bolometer detectors operate, and 1/f noise level is only drastic at low frequency.

The Noise Equivalent Power (NEP) is defined as incident infrared power on bolometer membrane that generates a signal equal to the root-mean-square noise. Therefore, if thermal fluctuation noise is the only noise present, as an ideal case, then the NEP of the bolometer is [7]

$$NEP = G \cdot \sqrt{\frac{KT^2}{C}} \tag{16}$$

where G is total thermal conductance.

The Detectivity (D^*) is defined as the root-mean-square signal to noise ratio of 1 Hz bandwidth per unit root-mean-square incident radiant power per square root bolometer membrane area. The Detectivity provides information that is equivalent to NEP, but with the possibility to compare bolometer pixels of the same type but with different pixel areas [1]. Thus it can be expressed as

$$D^* = \frac{\sqrt{A}}{NEP} \tag{17}$$

Therefore, we predict the figure of merit of our model as $D^* = 6.07\times10^8$ [cm.Hz$^{1/2}$.W^{-1}], which is in a good agreement with experimental reports. By combining of Eqs. (16), (17) and (7) we can obtain

$$D^* = \sqrt{\frac{A \cdot \tau}{G \cdot K \cdot T^2}} \tag{18}$$

This means the speed of a device cannot be increased without decreasing the sensitivity. By choosing the desired time constant by means of thermal capacitance adjusting, and using the smallest possible thermal conductance, the ultimate performance of the detector can be obtained.

5. Conclusion

The proposed calculation model makes it possible to estimate the resulting Detectivity of uncooled bolometer detector. We considered temperature dependence of thermal coefficient of resistance, thermal capacitance and thermal conductance through legs which result in more reliable outcomes.

The presented equivalent thermal circuit model simplifies the optimization of the design parameters of uncooled bolometer detectors. This analysis in also demonstrated that the bolometer detector operates in a background limited mode when there is no thermal conduction through legs and all energy exchanges with bolometer membrane are radiative.

We determined that the response time becomes longer as the Detectivity rises. Thus a bolometer detector cannot have a high Detectivity and a high speed at the same time. Based on VO_x parameters, our model predicted a D^* as 6.07×10^8 [cm.Hz$^{1/2}$.W^{-1}] which is in a good agreement compared with experimental cases.

References

[1] M. F. Niklaus, C. Jansson, A. Decharat, J.E. Källhammer, H. Pettersson and G. Stemme, in: Proceedings of SPIE, vol. 6542, pp.1L.1-1L.10, 2007.
[2] A. Rogalski, Opto-Electronics Review, vol.12, no.2, pp. 221–245,2004.

[3] R. V. Sudiwala, M. J. Griffin and A. L. Woodcraft, Int. J. Inf. Mill. Waves, vol. 23, no.4, pp. 545–573, 2002.
[4] P. Eriksson, J.Y. Andersson and G. Stemme, IEEE Journal of Microelectromechanical Systems, vol. 6, no. 1, pp. 55-61,1997.
[5] Yoshiki Tsujino, Infrared Physics & Technology, vol. 53, pp. 50–60, 2010.
[6] Adam L. Woodcraft et al., APPLIED OPTICS, vol. 42, no. 25, pp. 5009-5016, 2003.
[7] Paul W. Kruse and David D. Skatrud, in: Uncooled Infrared Imaging Arrays and Systems, vol. 47 of Semiconductors And Semimetals, chapter 3, Academic Press 2000.